Electronic Supplementary Material (ESI) for Dalton Transactions

Enhanced deep-blue emission from Pt(II) complexes bound to 2-pyridyltetrazolate and an *ortho*-xylene-linked bis(NHC)cyclophane

Karen D. M. MaGee, Phillip J. Wright, Sara Muzzioli, Claire Siedlovskas, Paolo Raiteri, Murray V. Baker, David H. Brown, Stefano Stagni,* Massimiliano Massi*

Supplementary Information

General experimental details

All reagents and solvents were purchased from Sigma Aldrich and used as received without further purification. Nuclear magnetic resonance spectra, consisting of ^{1}H, ^{13}C, and 2D-HSQC spectra were recorded using a Bruker Avance 400 spectrometer (400.1 MHz for ^{1}H, 100 MHz for ^{13}C) at 300 K. ^{1}H and ^{13}C chemical shifts were referenced to residual solvent signals. Electron Spray Ionization (ESI) mass spectra were obtained from a Waters ZQ-4000 instrument and acetonitrile was used as the solvent in each experiment. Melting points were determined using a BI Barnsted Electrothermal 9100 apparatus. Elemental analyses were obtained at the Central Science Laboratory, University of Tasmania, using a Thermo Finnigan EA 1112 Series Flash.

Absorption spectra were recorded at room temperature using a Perkin Elmer Lambda 35 UV/Vis spectrometer. Uncorrected steady state emission and excitation spectra were recorded on an Edinburgh FLSP920 spectrometer equipped with a 450 W Xenon arc lamp, double excitation and single emission monochromators and a peltier cooled Hamamatsu R928P photomultiplier tube (185-850 nm). Emission and excitation spectra were corrected for source intensity (lamp and grating) and emission spectral response (detector and grating) by a calibration curve supplied with the instrument. According to the approach described by Demas and Crosby,[1] luminescence quantum yields (Φ_{em}) were measured in optically dilute solutions (O.D. < 0.1 at excitation wavelength) obtained from absorption spectra on a wavelength scale [nm] and compared to the reference emitter by the following equation:

$$\Phi_x = \Phi_r \left[\frac{A_r(\lambda_r)}{A_x(\lambda_x)}\right]\left[\frac{I_r(\lambda_r)}{I_x(\lambda_x)}\right]\left[\frac{n_x^2}{n_r^2}\right]\left[\frac{D_x}{D_r}\right]$$

where A is the absorbance at the excitation wavelength (λ), I is the intensity of the excitation light at the excitation wavelength (λ), n is the refractive index of the solvent, D is the integrated intensity of the luminescence and Φ is the quantum yield. The subscripts r and x refer to the reference and the sample, respectively. The quantum yield determinations were performed at identical excitation wavelength for

the sample and the reference, therefore cancelling the $I(\lambda_r)/I(\lambda_x)$ term in the equation. All the Pt complexes were measured against an air-equilibrated water solution of $Ru(bpy)_3Cl_2$ used as reference (Φ_r = 0.028).[2] Emission lifetimes (τ) were determined with the single photon counting technique (TCSPC) with the same Edinburgh FLSP920 spectrometer using pulsed picosecond LEDs (EPLED 295 or EPLED 360, FHWM <800 ps) as the excitation source, with repetition rates between 10 kHz and 1 MHz, and the above-mentioned R928P PMT as detector. The goodness of fit was assessed by minimizing the reduced χ^2 function and by visual inspection of the weighted residuals. To record the 77 K luminescence spectra, the samples were put in quartz tubes (2 mm diameter) and inserted in a special quartz dewar filled with liquid nitrogen. The solvent (dichloromethane) used in the preparation of the solutions for the photophysical investigations was of spectrometric grade. All the prepared solutions were filtered through a 0.2 μm syringe filter before measurement. Degassed solutions were prepared by the freeze-pump-thaw technique. Experimental uncertainties are estimated to be ±8% for lifetime determinations, ±20% for quantum yields, ±2 nm and ±5 nm for absorption and emission peaks, respectively.

Time dependent density functional theory calculations were performed with GAUSSIAN 09[3] in order to calculate the absorption spectra of all compounds. Prior to these calculations the structures were relaxed at the 6-311g** level of theory. Pt atoms were treated with the Stuttgart-Dresden (SDD) Effective Core Potential and the effect of the solvent was mimicked with the PCM solvation model. The low lying singlet-singlet excitation energies were calculated at the same level of theory and the spectra were reproduced as the superposition of Gaussian functions with heights proportional to the calculated intensities and a variance of 11 nm.

Synthetic details

Synthesis of [Pt(cyph)(pytet)]PF_6

[Pt(**cyph**)Cl_2] (38.6 mg, 0.06 mmol) and **pytet**H (10.7 mg, 0.07 mmol) were dissolved in DMSO (4 mL) and heated up to 100 °C. Triethylammine (12 µL, 0.08 mmol) was added and the reaction was cooled slowly to room temperature and stirred overnight. The solution was concentrated under reduced pressure to approximately 1 mL. A saturated aqueous solution of KPF_6 (10 mL) was then added. The obtained precipitate was collected and purified via recrystallization from a $CHCl_3$/acetone mixture. Yield (41.2 mg, 79%); ^{1}H-NMR [$(CD_3)_2CO$), ppm]: δ = 5.31 (d, J = 14.4 Hz, 2H, 2 × C**H**H), 5.32 (d, J = 14.4 Hz, 2H, 2 × CH**H**), 6.90 (d, J = 14.4 Hz, 2H, 2 × C**H**H), 7.06 (d, J = 14.4 Hz, 2H, 2 × C**H**H), 7.49-7.43 (m, 4H, 4 × C**H** phenyl), 7.67 (s, 2H, 2 x C**H** imidazolyl), 7.72 (s, 2H, 2 x C**H** imidazolyl), 7.77-7.74 (m, 1H, C**H** pyridyl), 7.92-7.87 (m, 4H, 4 × C**H** phenyl), 8.54-8.42 (m, 3H, 3 × C**H** pyridyl); ^{13}C-NMR [$(CD_3)_2CO$), ppm]: δ = 52.8 (**C**H_2), 53.0 (**C**H_2), 122.9 (**C**H imidazolyl), 123.20 and 123.30 (**C**H imidazolyl and pyridyl), 128.2 (**C**H pyridyl), 130.9 (**C**H phenyl), 131.0 (**C**H phenyl), 133.5 (**C**H phenyl), 133.6 (**C**H phenyl), 136.4 (quater. **C** phenyl), 136.5 (quater. **C** phenyl), 142.7 (quater. **C** pyridyl), 143.2 (**C**H pyridyl), 148.9 (**C**-Pt imidazolyl), 149.2 (**C**-Pt imidazolyl), 153.1 (**C**H pyridyl), 166.0 (**C** tetrazole); ESI-MS (m/z) = 681 [M – (PF_6)]$^+$; Anal. Calcd. (%) for $C_{28}H_{24}N_9F_6PPt$: C 40.68, H 2.93, N 15.25. Found: C 40.41, H 2.72, N 15.25.

Synthesis of [Pt(cyph)(pytetMe)](PF_6)(OTf)

[Pt(**cyph**)(**pytet**)]PF_6 (15.4 mg, 0.02 mmol) in dichloromethane (2 mL) was cooled in a cryogenic bath of acetone and liquid nitrogen. Methyl triflate (600 µL, 0.1 M solution in DCM) was added. The solution was kept in the cold bath for 1 hour and then allowed to warm up to room temperature. The reaction was then stirred overnight at room temperature. The solvents were removed under reduced pressure and the remaining solids were washed with water, diethyl ether and eventually dried in air. Yield (14.0 mg, 63%); ^{1}H-NMR [$(CD_3)_2CO$), ppm]: δ = 4.78 (s, 3H, C**H**$_3$), 5.37 (2 overlapping d, J = 14.8 Hz, 4H, 2 × C**HH**), 6.88 (d, J = 14.0 Hz, 2H, 2 × C**H**H), 6.92 (d, J = 14.0 Hz, 2H, 2 × CH**H**), 7.49-7.45 (m, 4H, 4 x C**H** phenyl), 7.75 (s, 2H, 2 x C**H** imidazolyl), 7.77 (s, 2H, 2 x C**H** imidazolyl), 7.92-7.88 (m, 4H, 4 x C**H** phenyl), 8.05-8.02 (m, 1H, C**H** pyridyl), 8.71-8.66 (m, 3H, 3 x C**H** pyridyl). ^{13}C-NMR

[$(CD_3)_2CO$), ppm]: δ = 43.1 (**C**H_3), 52.7 (**C**H_2), 52.9 (**C**H_2), 123.7 (**C**H, imidazolyl), 123.9 (**C**H, imidazolyl), 125.4 (**C**H pyridyl), 131.2 (2 x **C**H phenyl), 131.4 (**C**H pyridyl), 133.6 (2 x **C**H phenyl), 136.0 (quater. **C** phenyl), 136.1 (quater. **C** phenyl), 142.5 (**C**-Pt imidazolyl), 144.2 (**C**H pyridyl), 144.9 (**C**-Pt imidazolyl), 154.2 (**C**H pyridyl) (quaternary C on pyridyl and tetrazole not clearly distinguishable). ESI-MS (*m*/*z*) = 348 $[M – (PF_6)(OTf)]^{2+}$; Anal. Calcd. (%) for $C_{29}H_{27}N_9F_9O_3PPtS$: C 36.37, H 2.75, N 12.73. Found: C 36.18, H 2.42, N 12.52.

NMR spectra

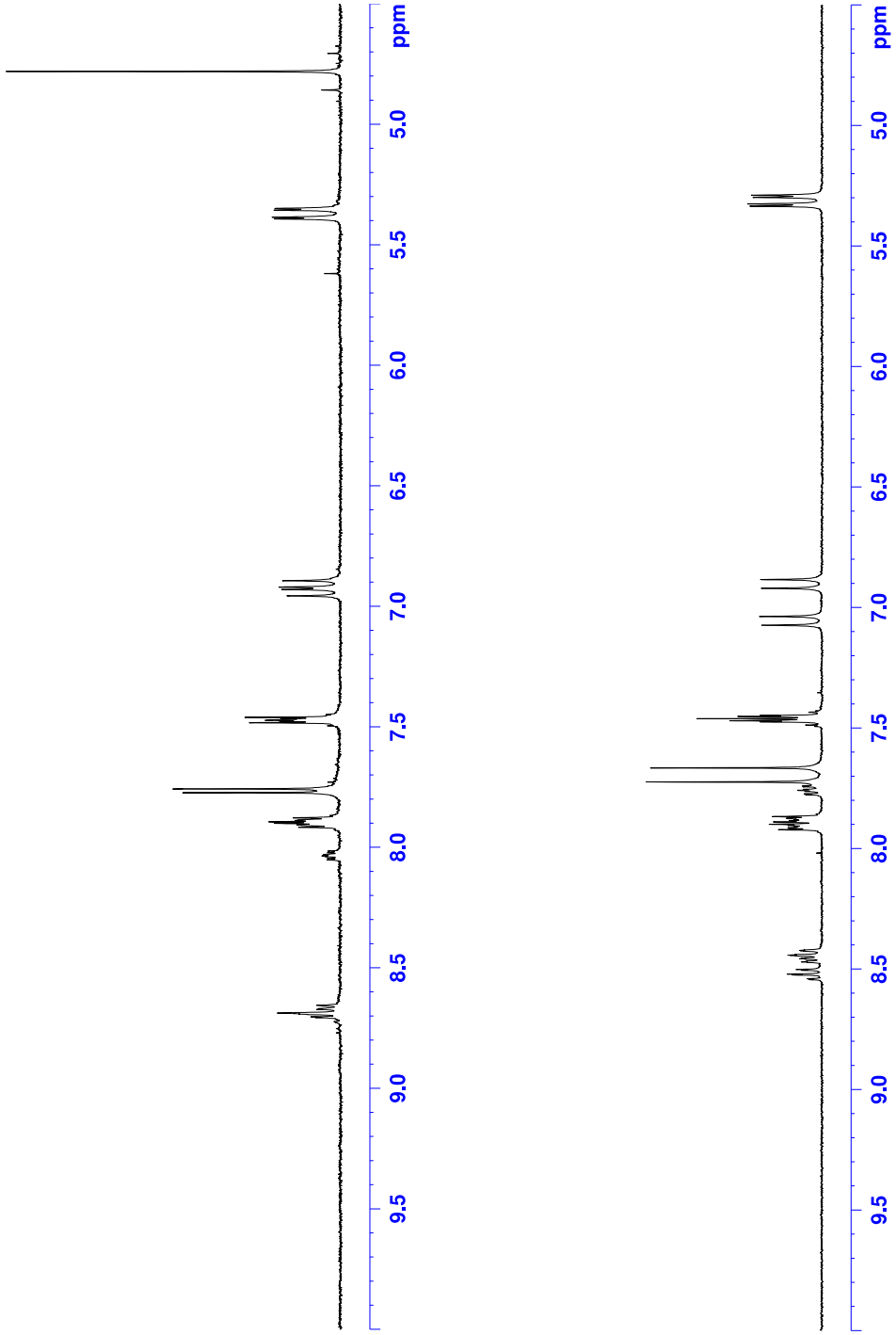

^{1}H-NMR spectra of [Pt(**cyph**)(**pytet**Me)](PF$_6$)(OTf) (top) and [Pt(**cyph**)(**pytet**)](PF$_6$) (bottom).

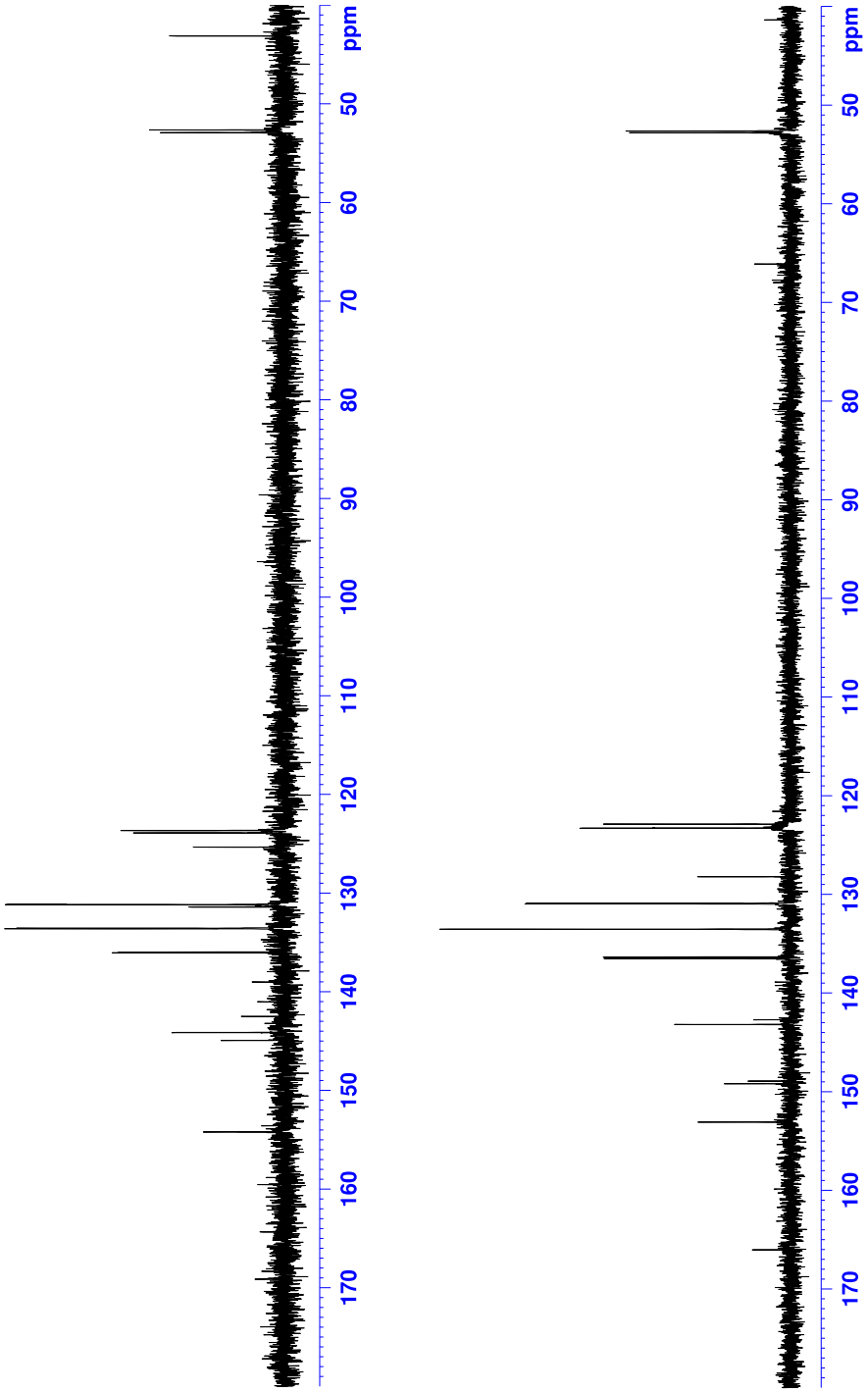

^{13}C-NMR spectra of [Pt(**cyph**)(**pytet**Me)](PF$_6$)(OTf) (top) and [Pt(**cyph**)(**pytet**)](PF$_6$) (bottom).

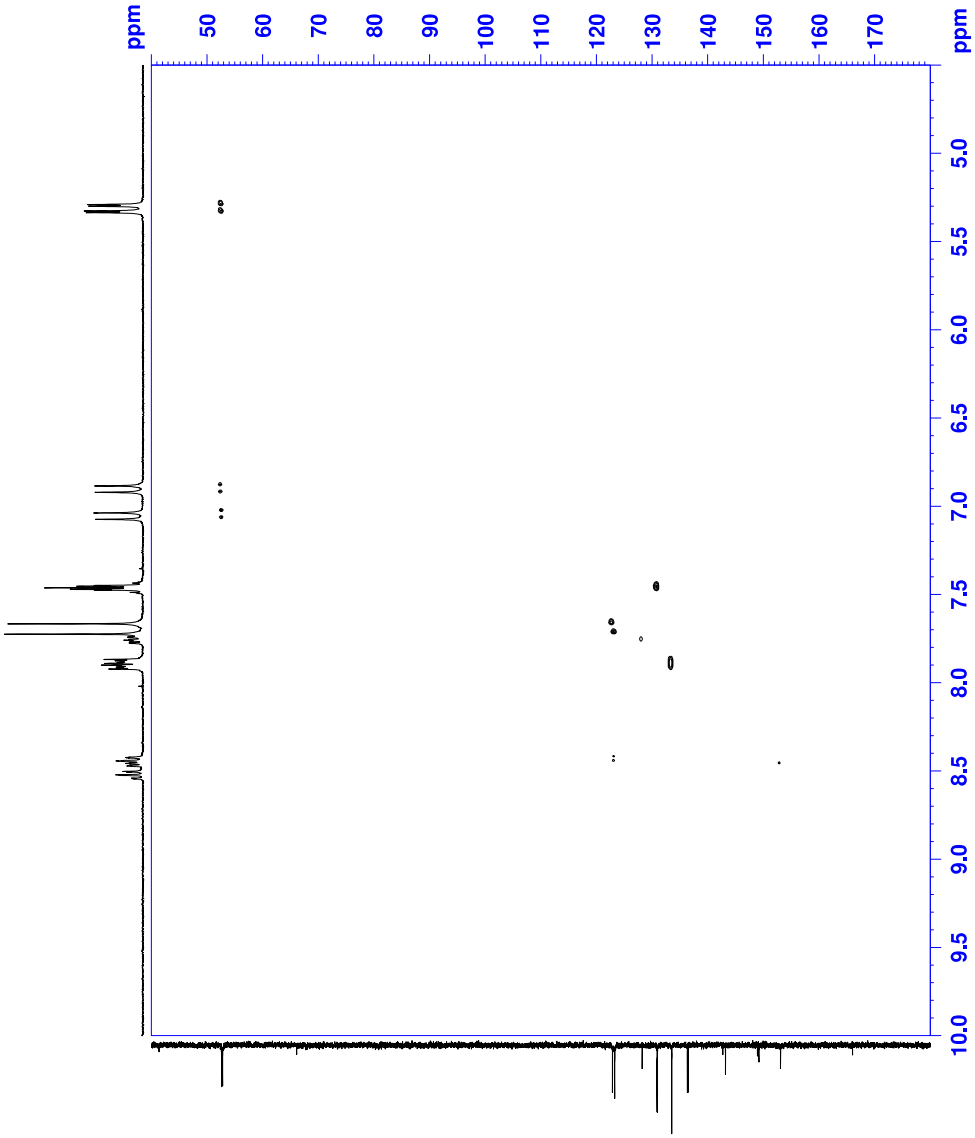

HSQC spectrum of [Pt(**cyph**)(**pytet**)](PF_6).

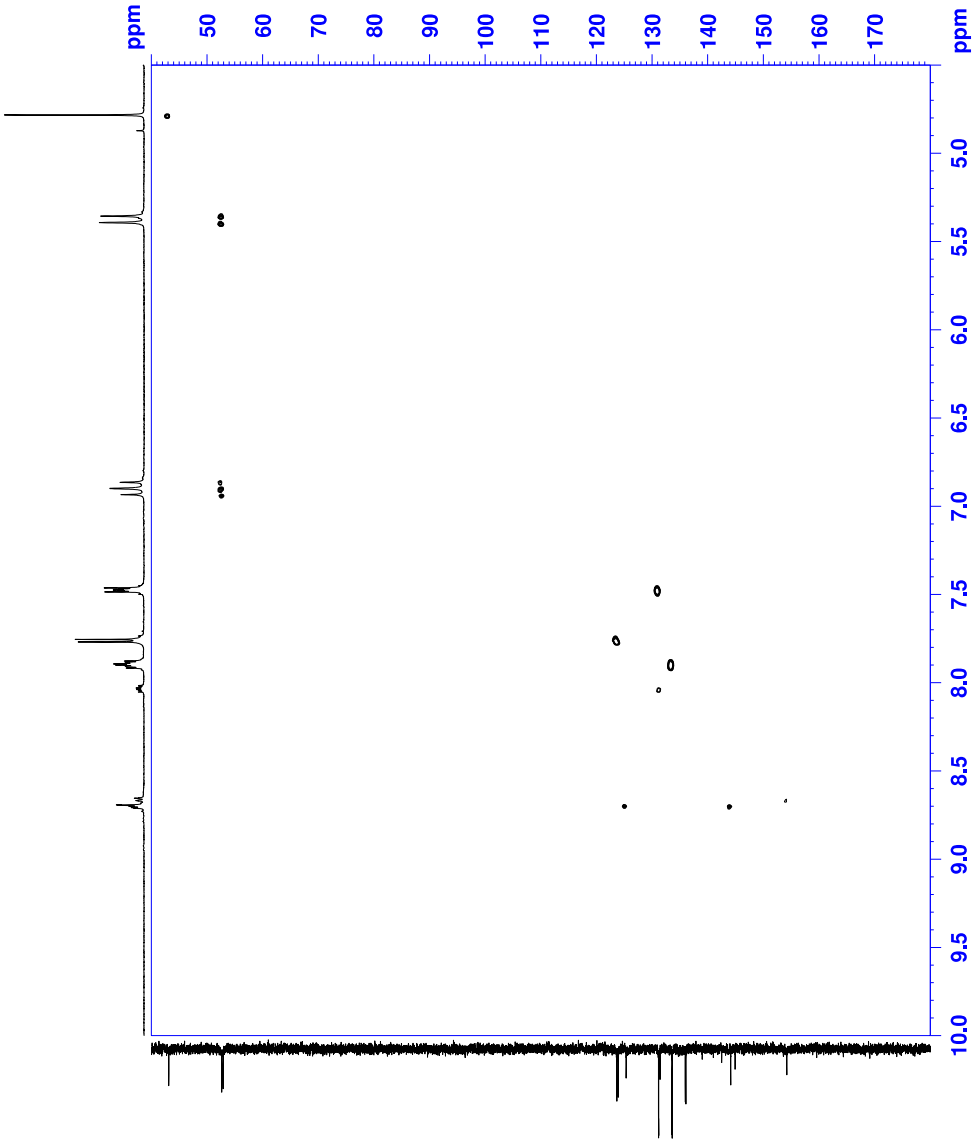

HSQC spectrum of [Pt(**cyph**)(**pytetMe**)](PF_6)(OTf).

Structure of the Complexes

Despite numerous crystallization attempts using a variety of procedures (e.g. double layers, slow evaporation, vapour diffusion), we could not obtain single crystals suitable for X-ray diffraction. Both complexes were always collected as amorphous powders or finely dispersed polycrystalline solids. The spectroscopic data on the [Pt(**cyph**)(**pytet**)]PF_6 complex confirm that the ligand **pytet** is bound via the two N atoms on the pyridine and tetrazole rings, thus excluding the formation of the linkage isomer formed by cyclometallation of the pyridine ring. This η^2-(N,N') binding mode is confirmed by the four distinct pyridyl H environments in the NMR spectrum. On the other hand for [Pt(**cyph**)(**pytetMe**)]$^{2+}$, the methylation is proposed to occur predominantly on the N3 atom of the tetrazole ring, since the NMR spectrum shows a signal at 4.78 ppm corresponding to the CH_3 substituent. The NMR spectrum also shows a minor peak at around 4.88 ppm that could be due to a small fraction of the methylation occurring on the N2 position. Methylation of the N4 atom is excluded due to steric hindrance with the adjacent H atom on the pyridine ring and the absence of torsional freedom between the two rings caused by the coordination to the Pt center. No trace of products deriving from any eventual oxidative additions mechanism was detected from the NMR characterisation of the batches of the methylated species [Pt(**cyph**)(**pytetMe**)]$^{2+}$.

Photophysical data

Summary of the photophysical data

Complex	λ_{abs} ($10^3\varepsilon$) [nm ($M^{-1}cm^{-1}$)]	λ_{em} [nm]	τ [μs]	Φ
[Pt(**cyph**)(**pytet**)]$^+$ DCM, air	287 (9.31) 315 (3.74)	436	2.32	0.08
[Pt(**cyph**)(**pytet**)]$^+$ DCM, dear.	287 (9.31) 315 (3.74)	436	3.57	0.14
[Pt(**cyph**)(**pytet**)]$^+$ DCM, 77 K		432	47.82 (66%) 64.57 (34%)	
[Pt(**cyph**)(**pytet**)]$^+$ solid state		438	32.23 (44%) 53.84 (56%)	
[Pt(**cyph**)(**pytet**Me)]$^{2+}$ DCM, air	286 (9.73)	448	0.40	0.02
[Pt(**cyph**)(**pytet**Me)]$^{2+}$ DCM, dear.	286 (9.73)	448	0.39	0.02
[Pt(**cyph**)(**pytet**Me)]$^{2+}$ DCM, 77 K		422	30.79 (32%) 91.90 (68%)	
[Pt(**cyph**)(**pytet**Me)]$^{2+}$ solid state		448	10.41 (37%) 32.72 (63%)	

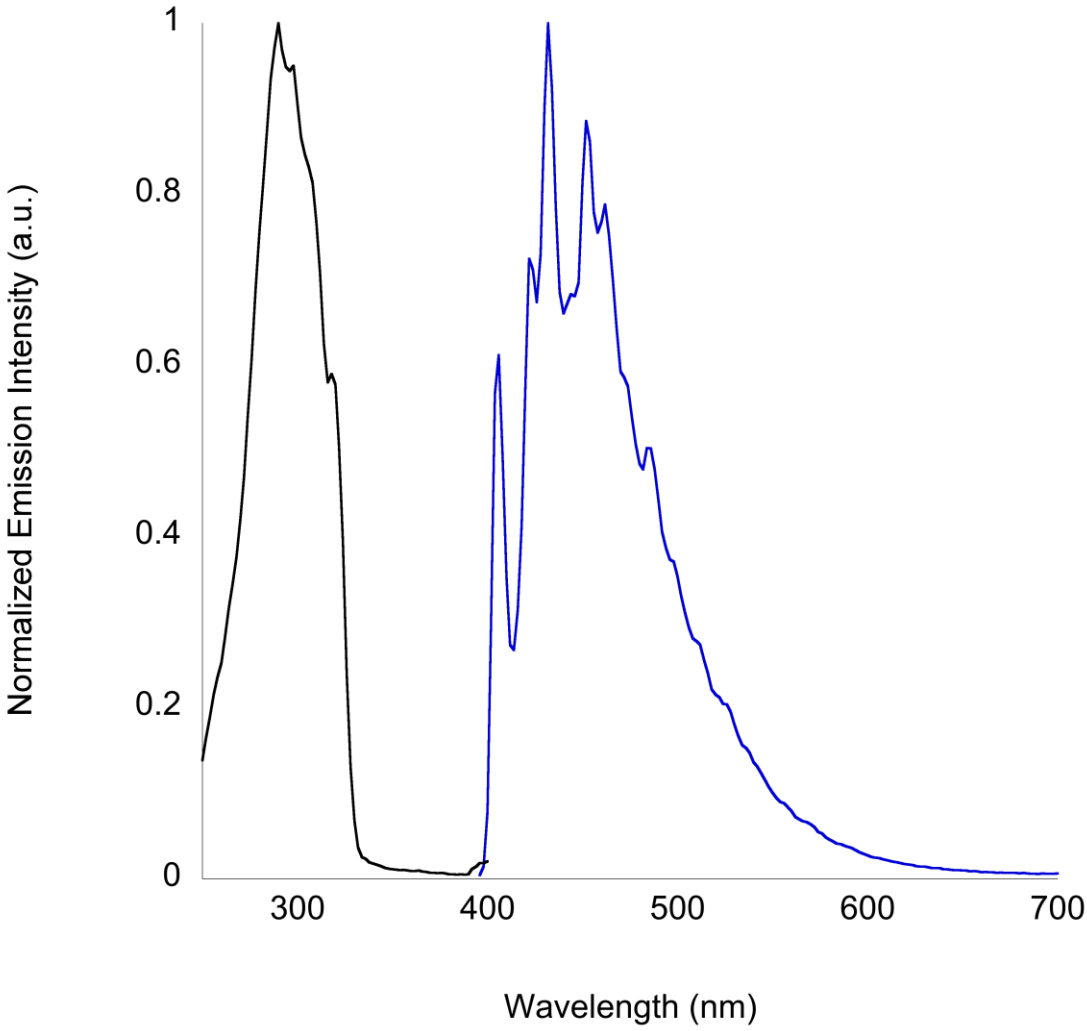

Excitation and emission profiles for [Pt(**cyph**)(**pytet**)]PF_6 from a ca. 10^{-5} M dichloromethane solution at 77 K.

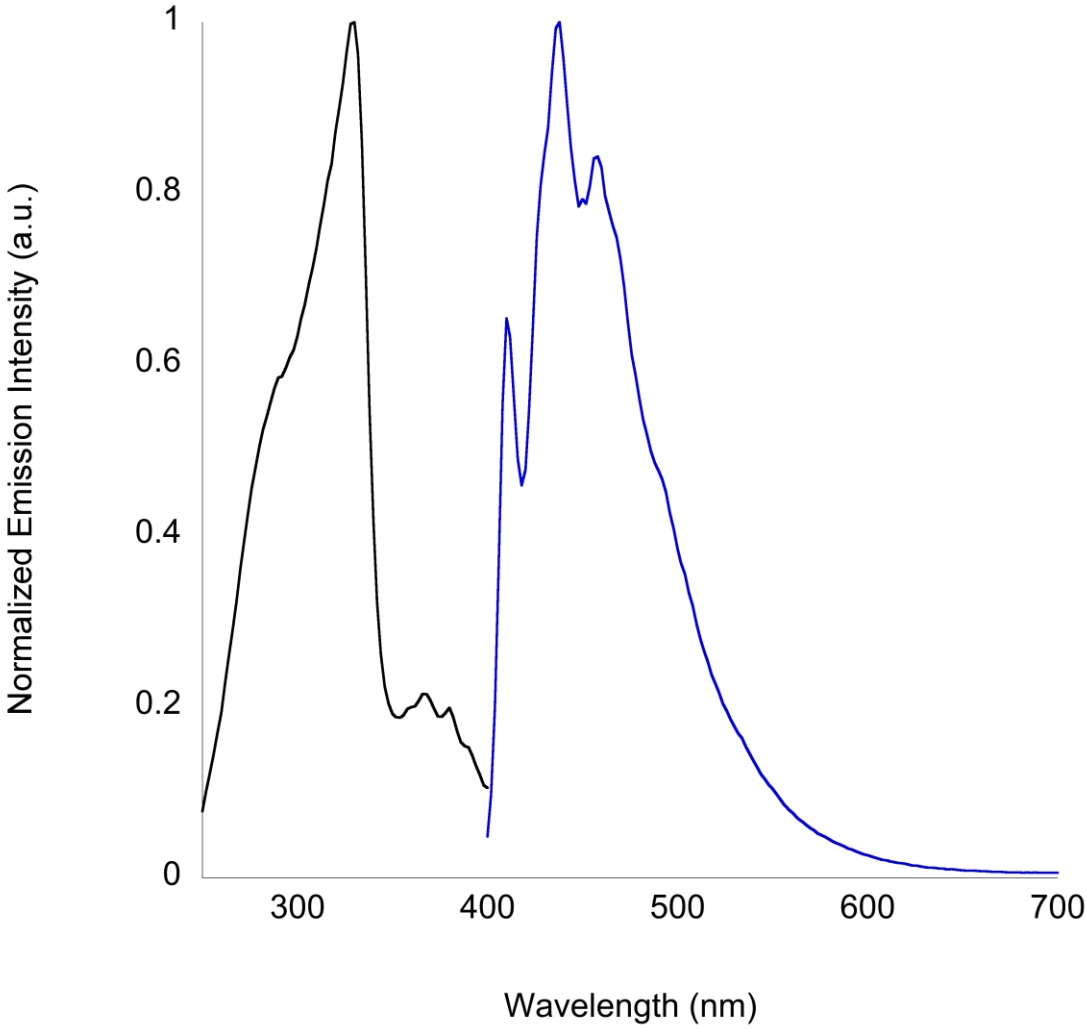

Excitation and emission profiles for [Pt(**cyph**)(**pytet**)]PF_6 from a solid sample.

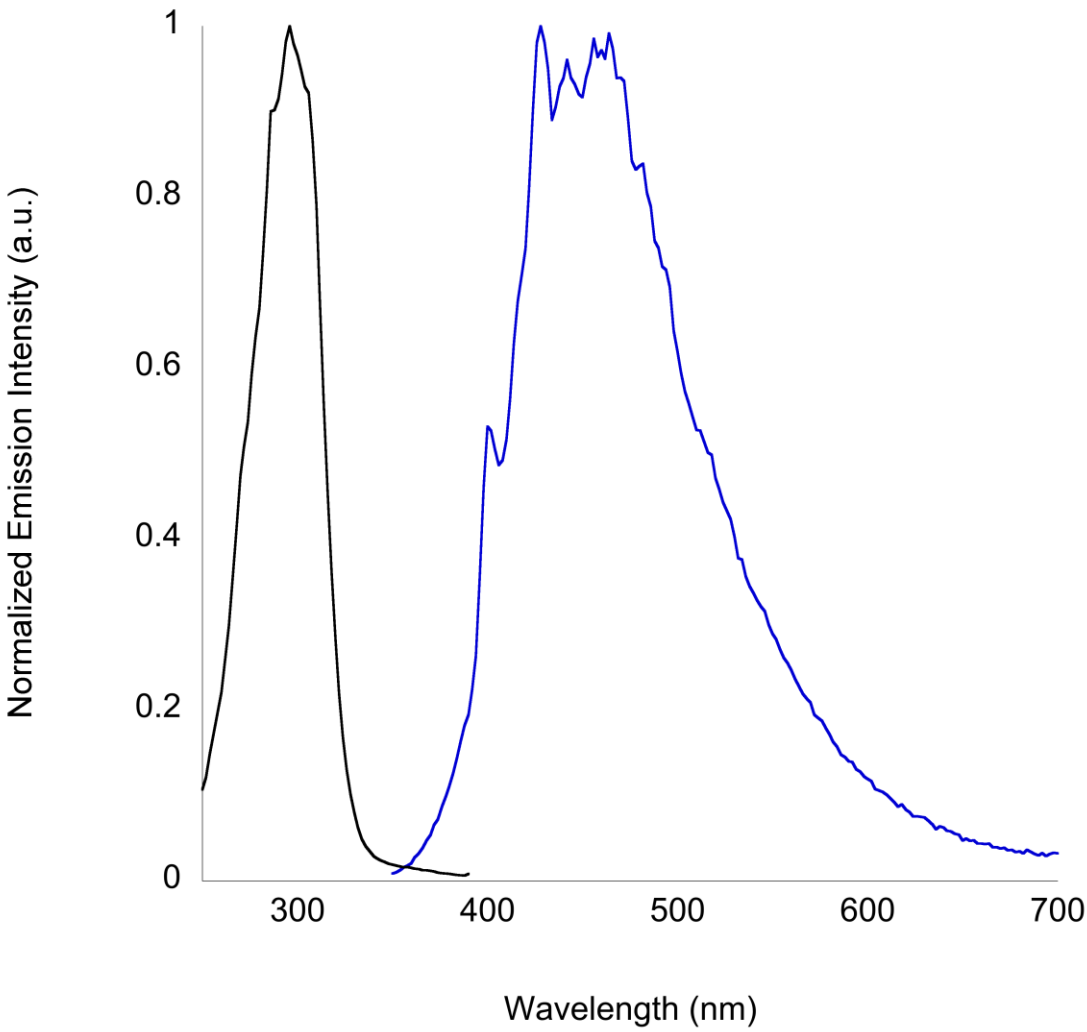

Excitation and emission profiles for [Pt(**cyph**)(**pytetMe**)](PF_6)(OTf) from a ca. 10^{-5} M dichloromethane solution at 77 K.

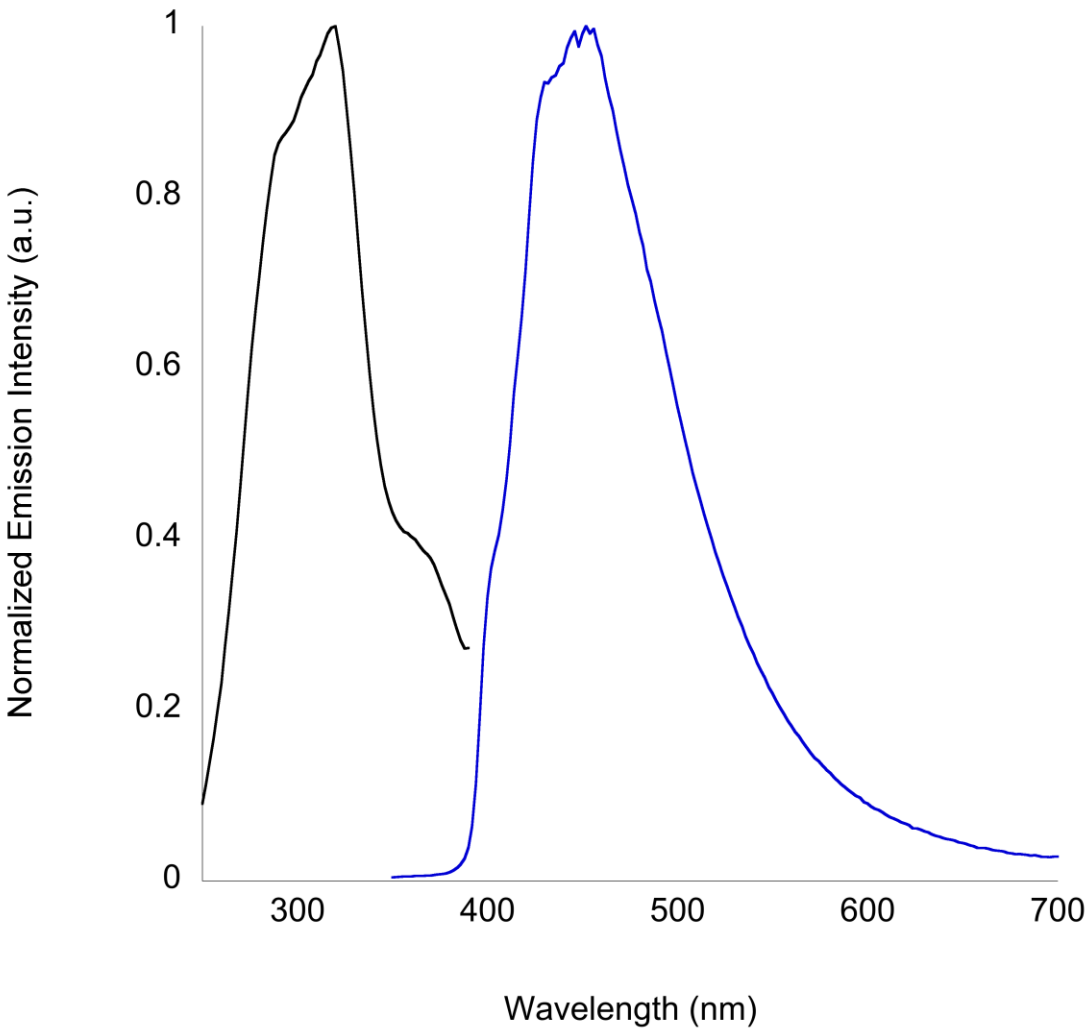

Excitation and emission profiles for [Pt(**cyph**)(**pytetMe**)](PF_6)(OTf) from a solid sample.

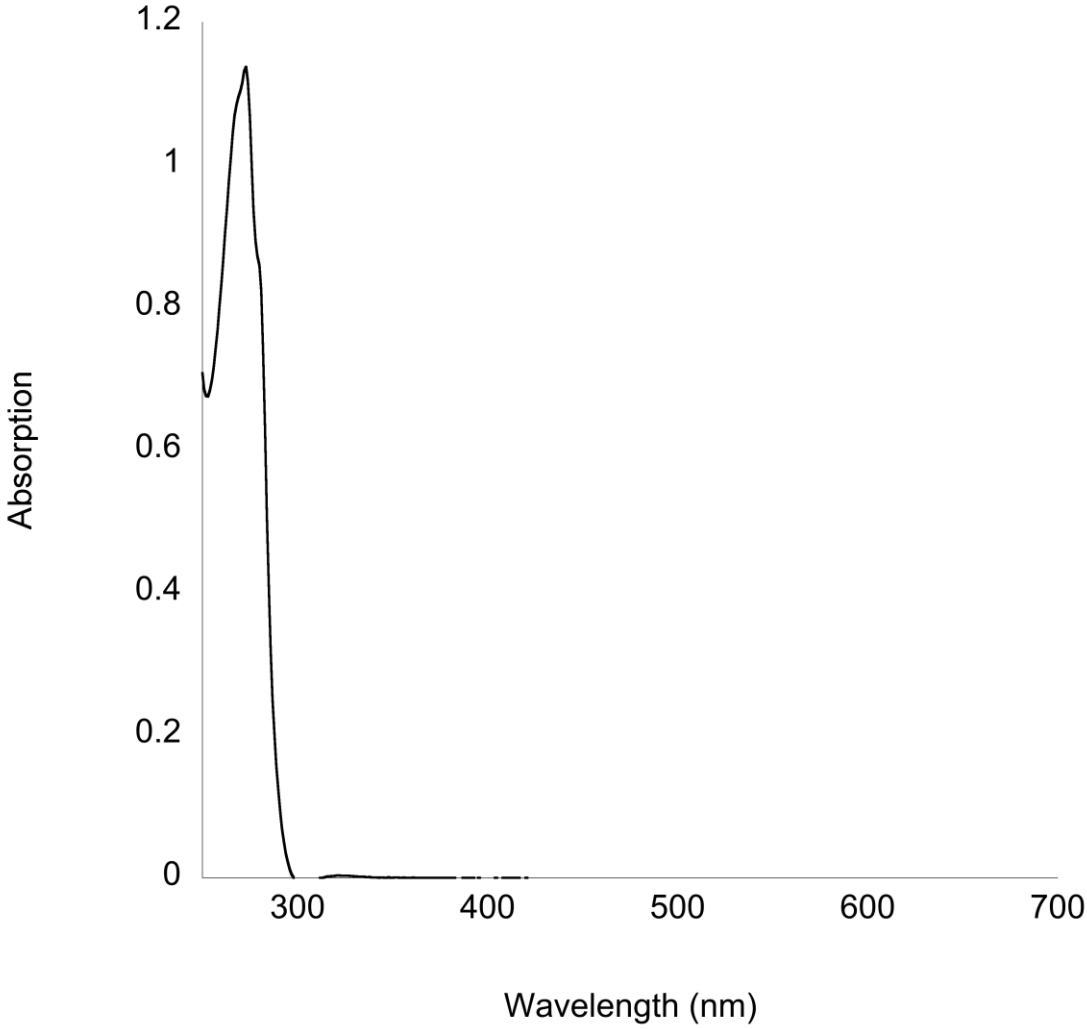

Absorption profile for an ethanol solution of **pytet**H.

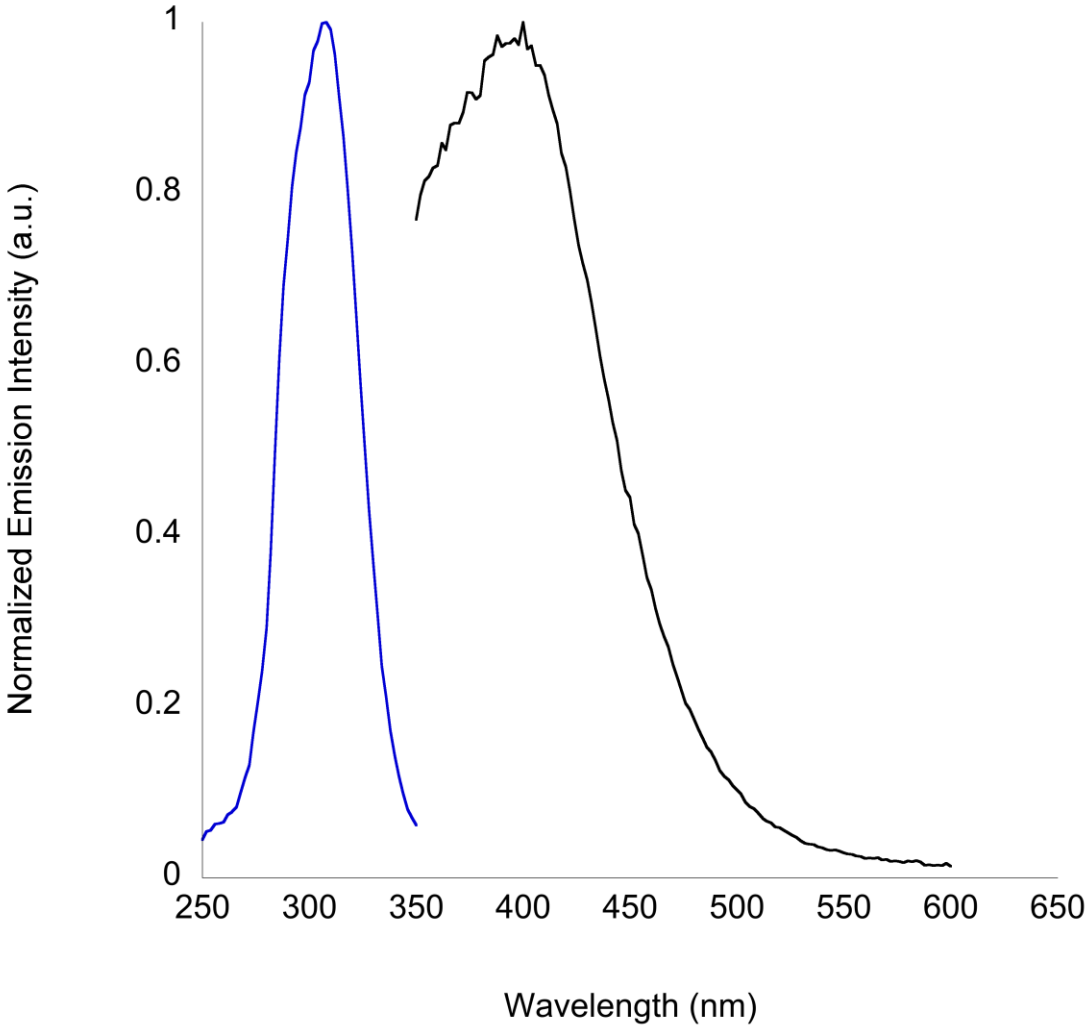

Excitation and emission profiles for **pytet**H from a ca. 10^{-5} M ethanol solution at room temperature.

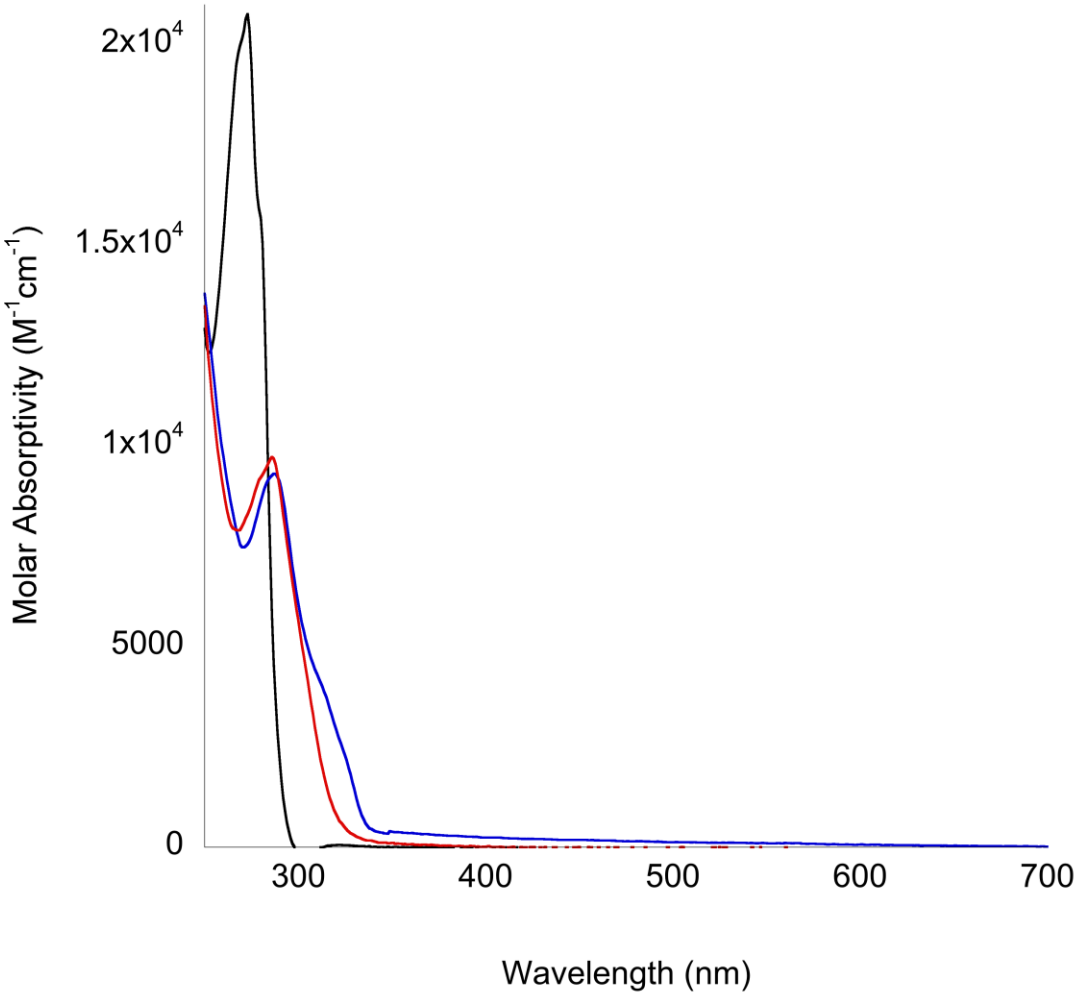

Overlay of the absorption plots for **pytet**H (black), [Pt(**cyph**)(**pytet**)]PF_6 (blue) and [Pt(**cyph**)(**pytetMe**)](PF_6)(OTf) (red).

CIE Coordinates

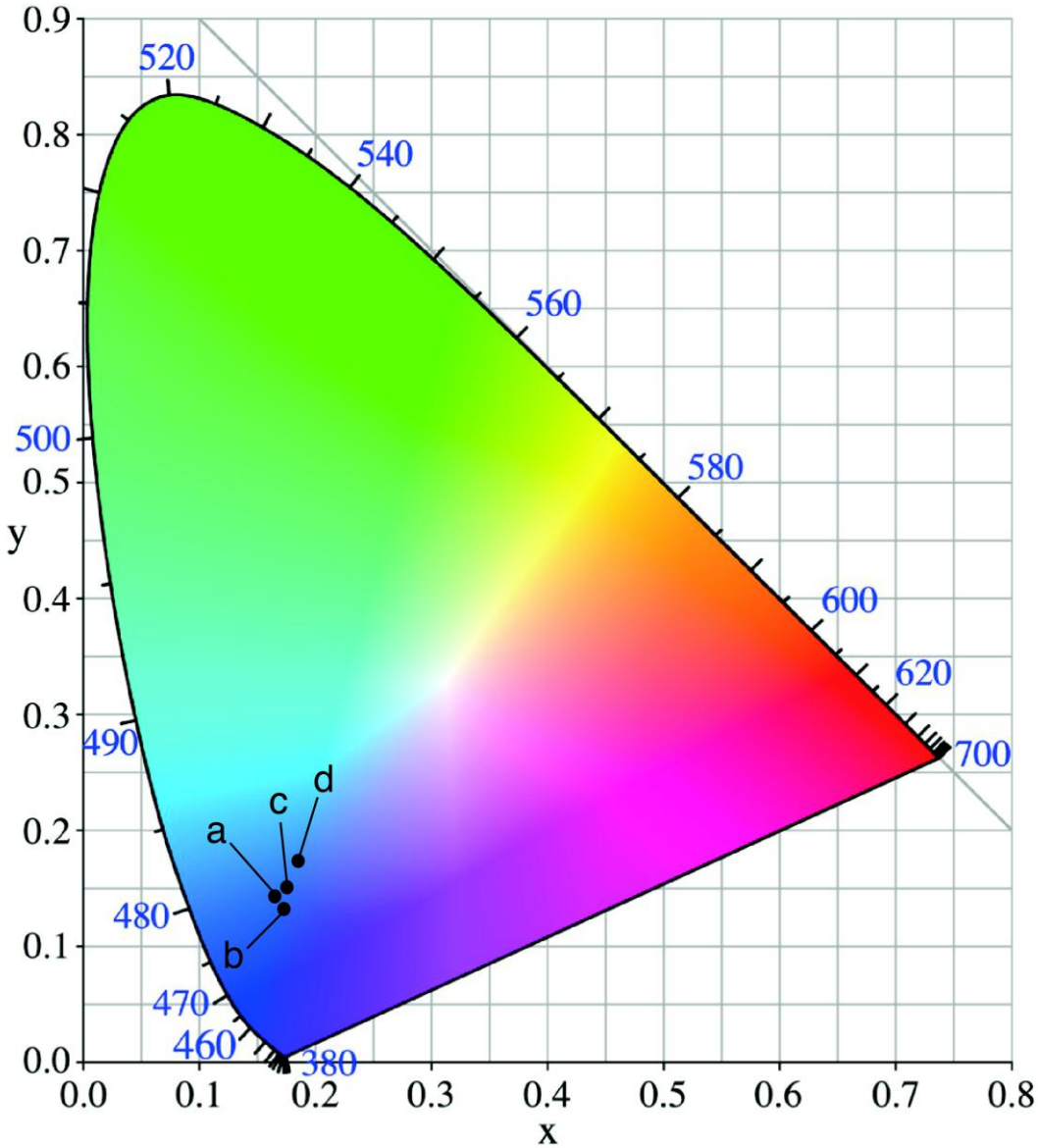

CIE coordinates for: a) [Pt(**cyph**)(**pytet**)]PF_6 in dichloromethane solution; b) [Pt(**cyph**)(**pytet**)]PF_6 in solid state; c) [Pt(**cyph**)(**pytetMe**)](PF_6)(OTf) in dichloromethane solution; d) [Pt(**cyph**)(**pytetMe**)](PF_6)(OTf) in solid state.

Computational calculations

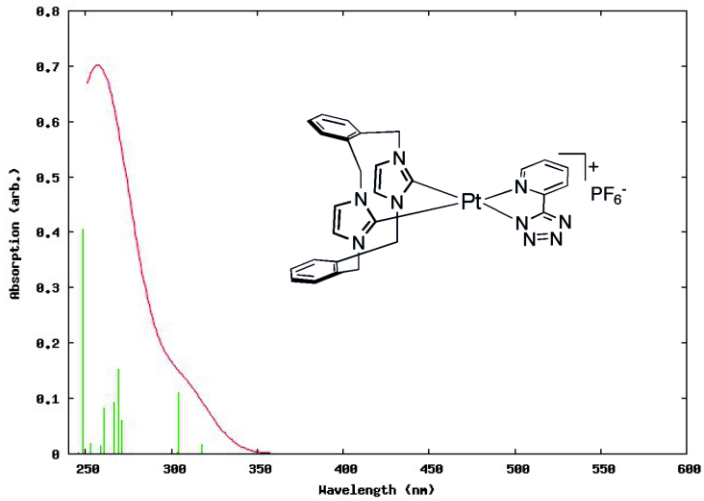

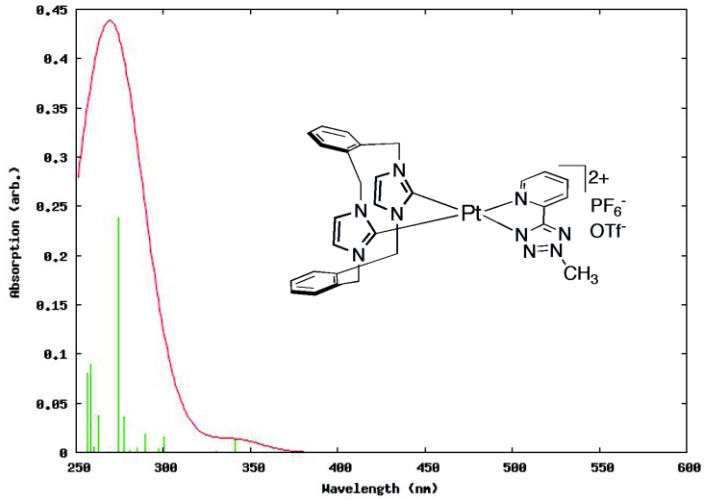

Simulated absorption spectra.

Calculated transitions for [Pt(**cyph**)(**pytet**)]$^{+}$

Wavelength	Intensity	Levels	Character
317.86 nm	0.0164	HOMO-1 -> LUMO	72.7 %
		HOMO -> LUMO	25.4 %
304.00 nm	0.1096	HOMO-8 -> LUMO	4.3 %
		HOMO-2 -> LUMO	93.2 %
303.25 nm	0.0011	HOMO-3 -> LUMO	2.0 %
		HOMO-1 -> LUMO	24.3 %
		HOMO -> LUMO	71.9 %
281.17 nm	0.0000	HOMO-3 -> LUMO	96.1 %
270.79 nm	0.0607	HOMO-9 -> LUMO	19.3 %
		HOMO-8 -> LUMO	13.5 %
		HOMO-5 -> LUMO	4.8 %
		HOMO-2 -> LUMO+1	3.6 %
		HOMO-1 -> LUMO+2	13.4 %
		HOMO-1 -> LUMO+3	6.2 %
		HOMO-1 -> LUMO+6	20.0 %
		HOMO -> LUMO+2	4.0 %
		HOMO -> LUMO+6	5.8 %
269.23 nm	0.1518	HOMO-8 -> LUMO	50.8 %
		HOMO-5 -> LUMO	6.9 %
		HOMO-4 -> LUMO	9.9 %
		HOMO-2 -> LUMO+1	2.1 %
		HOMO-1 -> LUMO+2	6.6 %
		HOMO-1 -> LUMO+3	3.2 %
		HOMO-1 -> LUMO+6	9.2 %
		HOMO -> LUMO+2	2.1 %
		HOMO -> LUMO+6	2.7 %
266.37 nm	0.0919	HOMO-9 -> LUMO	17.1 %
		HOMO-4 -> LUMO	62.4 %
		HOMO-1 -> LUMO+2	4.0 %
		HOMO-1 -> LUMO+6	5.5 %
		HOMO -> LUMO+2	2.0 %
		HOMO -> LUMO+6	2.2 %
262.26 nm	0.0004	HOMO-10 -> LUMO	91.1 %
260.99 nm	0.0819	HOMO-9 -> LUMO	28.7 %
		HOMO-8 -> LUMO	26.5 %
		HOMO-5 -> LUMO	16.3 %
		HOMO-4 -> LUMO	22.6 %

260.47 nm	0.0000	HOMO-1 -> LUMO+1	69.0 %
		HOMO -> LUMO+1	29.1 %
258.99 nm	0.0133	HOMO-9 -> LUMO	20.1 %
		HOMO-5 -> LUMO	70.4 %
		HOMO-4 -> LUMO	3.7 %
		HOMO-2 -> LUMO+1	3.6 %
256.57 nm	0.0010	HOMO-7 -> LUMO	52.6 %
		HOMO-6 -> LUMO	43.4 %
255.71 nm	0.0000	HOMO-7 -> LUMO	45.1 %
		HOMO-6 -> LUMO	52.5 %
253.26 nm	0.0183	HOMO-1 -> LUMO+2	11.5 %
		HOMO-1 -> LUMO+6	8.7 %
		HOMO -> LUMO+2	41.4 %
		HOMO -> LUMO+3	6.0 %
		HOMO -> LUMO+6	21.5 %
252.14 nm	0.0000	HOMO-3 -> LUMO+1	4.0 %
		HOMO-1 -> LUMO+1	25.9 %
		HOMO -> LUMO+1	65.0 %
248.69 nm	0.4047	HOMO-9 -> LUMO	9.4 %
		HOMO-8 -> LUMO+1	4.3 %
		HOMO-2 -> LUMO+1	79.1 %
248.55 nm	0.0027	HOMO-8 -> LUMO+2	7.3 %
		HOMO-8 -> LUMO+3	3.8 %
		HOMO-8 -> LUMO+6	12.1 %
		HOMO-2 -> LUMO+2	29.4 %
		HOMO-2 -> LUMO+3	9.0 %
		HOMO-2 -> LUMO+6	29.1 %
246.12 nm	0.0013	HOMO-11 -> LUMO	91.9 %
		HOMO-10 -> LUMO	2.4 %
239.74 nm	0.0026	HOMO -> LUMO+2	46.1 %
		HOMO -> LUMO+3	18.3 %
		HOMO -> LUMO+6	26.8 %
238.51 nm	0.0010	HOMO-5 -> LUMO+2	2.3 %
		HOMO-3 -> LUMO+1	87.1 %
		HOMO -> LUMO+1	2.9 %
		HOMO -> LUMO+1	2.9 %

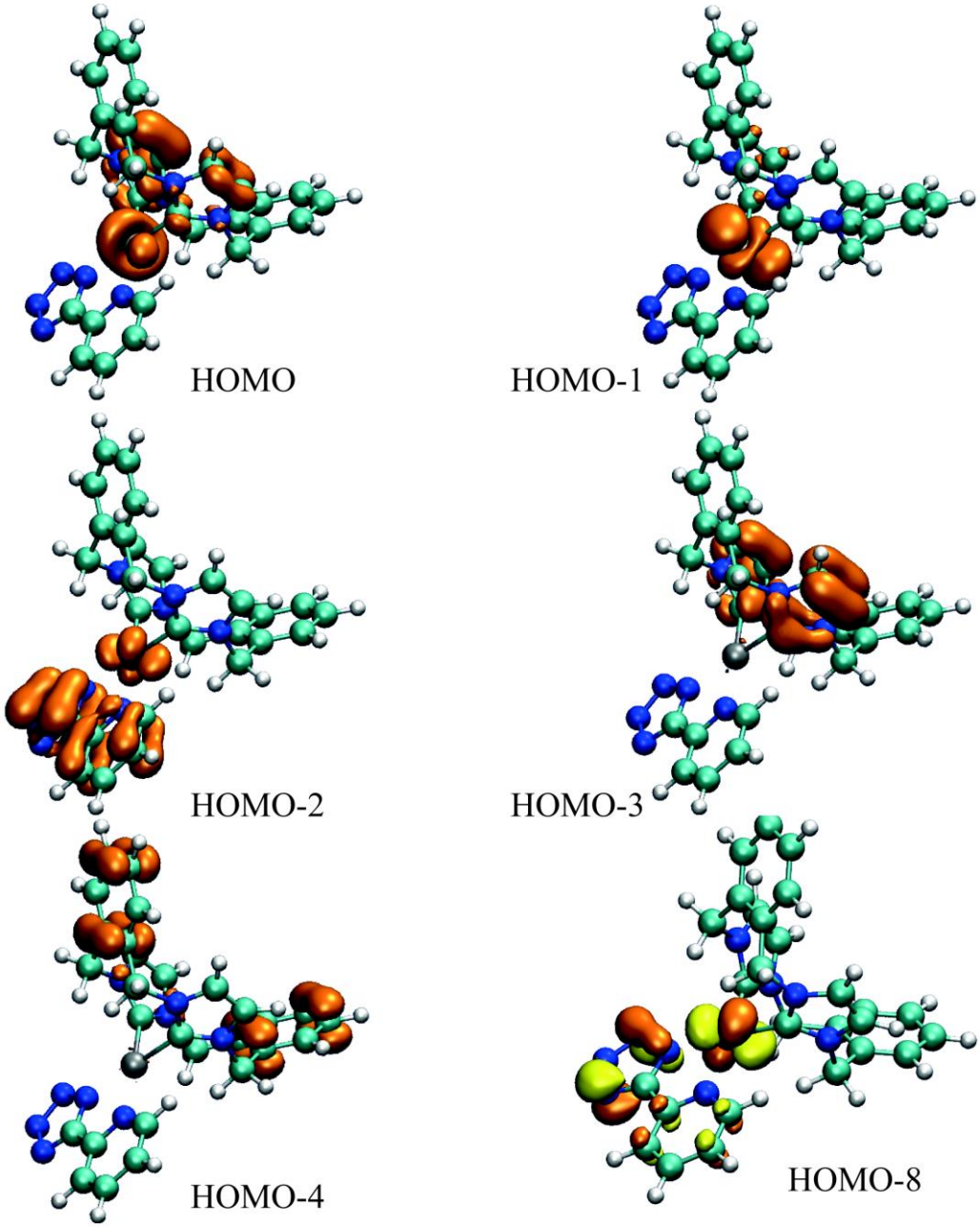

Selected occupied orbital representations for [Pt(**cyph**)(**pytet**)]$^{+}$.

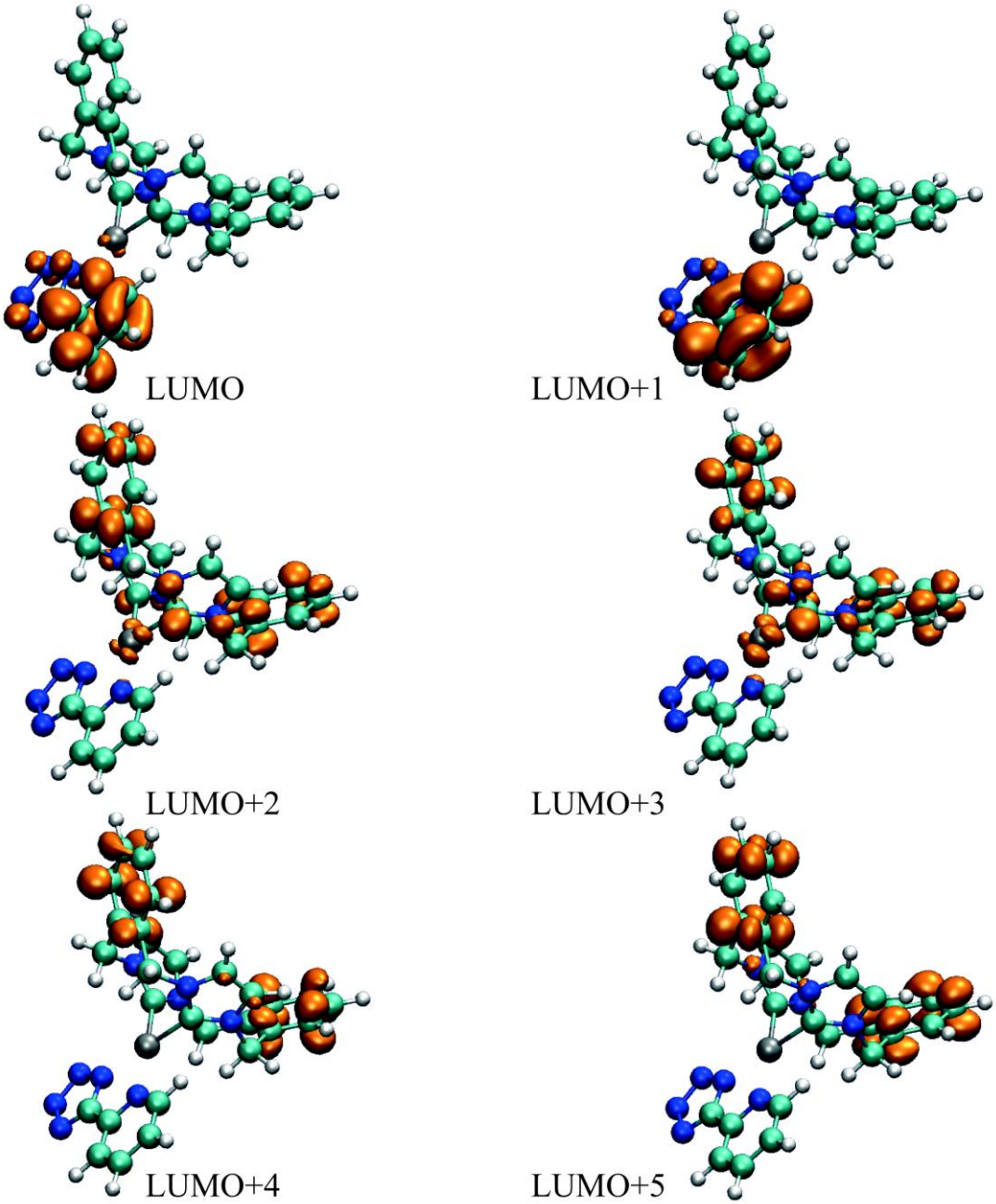

Selected unoccupied orbital representations for [Pt(**cyph**)(**pytet**)]$^{+}$.

Calculated transitions for [Pt(**cyph**)(**pytetMe**)]$^{2+}$

Wavelength	Intensity	Levels	Character
341.44 nm	0.0120	HOMO-6 -> LUMO	12.1 %
		HOMO-2 -> LUMO	63.7 %
		HOMO-1 -> LUMO	7.5 %
		HOMO -> LUMO	15.4 %
330.47 nm	0.0016	HOMO-6 -> LUMO	2.6 %
		HOMO-2 -> LUMO	15.1 %
		HOMO -> LUMO	80.4 %
312.75 nm	0.0000	HOMO-5 -> LUMO	3.4 %
		HOMO-2 -> LUMO	5.6 %
		HOMO-1 -> LUMO	87.7 %
		HOMO -> LUMO	2.7 %
300.31 nm	0.0162	HOMO-3 -> LUMO	97.8 %
297.14 nm	0.0034	HOMO-7 -> LUMO	19.3 %
		HOMO-4 -> LUMO	75.3 %
289.82 nm	0.0002	HOMO-6 -> LUMO	82.9 %
		HOMO-2 -> LUMO	14.9 %
289.66 nm	0.0186	HOMO-9 -> LUMO	2.9 %
		HOMO-7 -> LUMO	65.4 %
		HOMO-4 -> LUMO	23.6 %
		HOMO-2 -> LUMO+3	2.2 %
288.86 nm	0.0000	HOMO-5 -> LUMO	96.1 %
		HOMO-1 -> LUMO	3.3 %
285.28 nm	0.0048	HOMO-6 -> LUMO+1	7.8 %
		HOMO-2 -> LUMO+1	51.8 %
		HOMO-1 -> LUMO+1	4.2 %
		HOMO -> LUMO+1	32.5 %
280.53 nm	0.0019	HOMO-6 -> LUMO+1	4.4 %
		HOMO-2 -> LUMO+1	23.9 %
		HOMO-1 -> LUMO+1	4.5 %
		HOMO -> LUMO+1	64.3 %
277.50 nm	0.0359	HOMO-8 -> LUMO	12.0 %
		HOMO-7 -> LUMO	6.5 %
		HOMO-6 -> LUMO+3	10.9 %
		HOMO-6 -> LUMO+4	3.5 %
		HOMO-2 -> LUMO+3	41.1 %

		HOMO-2 -> LUMO+4	10.6 %
		HOMO-1 -> LUMO+3	3.6 %
		HOMO -> LUMO+3	5.0 %
274.53 nm	0.2375	HOMO-8 -> LUMO	79.5 %
		HOMO-2 -> LUMO+3	6.9 %
268.77 nm	0.0000	HOMO-5 -> LUMO+1	2.8 %
		HOMO-2 -> LUMO+1	8.7 %
		HOMO-1 -> LUMO+1	82.7 %
		HOMO -> LUMO+2	4.4 %
263.72 nm	0.0004	HOMO-6 -> LUMO+2	10.3 %
		HOMO-2 -> LUMO+1	2.0 %
		HOMO-2 -> LUMO+2	59.1 %
		HOMO-1 -> LUMO+2	8.3 %
		HOMO -> LUMO+2	19.2 %
262.65 nm	0.0370	HOMO-2 -> LUMO+3	5.7 %
		HOMO -> LUMO+3	69.5 %
		HOMO -> LUMO+4	13.0 %
260.06 nm	0.0059	HOMO-3 -> LUMO+1	98.5 %
258.37 nm	0.0893	HOMO-9 -> LUMO	60.9 %
		HOMO-7 -> LUMO+1	11.3 %
		HOMO-4 -> LUMO+1	19.7 %
258.29 nm	0.0000	HOMO-6 -> LUMO+2	3.0 %
		HOMO-2 -> LUMO+2	21.1 %
		HOMO-1 -> LUMO+1	3.7 %
		HOMO -> LUMO+2	0.0 %
256.19 nm	0.0806	HOMO-9 -> LUMO	19.3 %
		HOMO-4 -> LUMO+1	77.4 %
252.04 nm	0.0000	HOMO-6 -> LUMO+1	83.4 %
		HOMO-5 -> LUMO+1	3.0 %
		HOMO-2 -> LUMO+1	11.8 %
		HOMO-2 -> LUMO+1	11.8 %

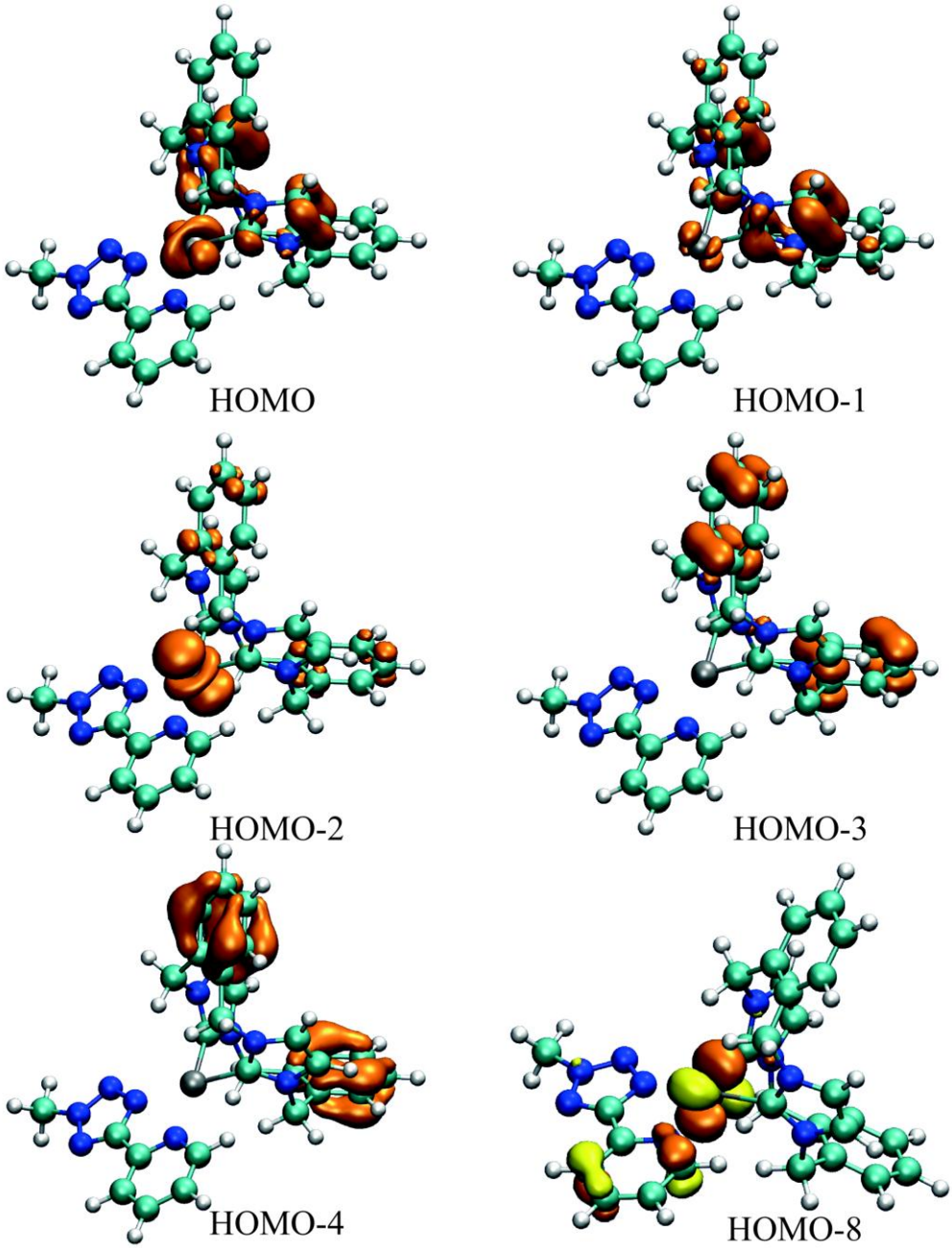

Selected occupied orbital representations for [Pt(**cyph**)(**pytetMe**)]$^{2+}$.

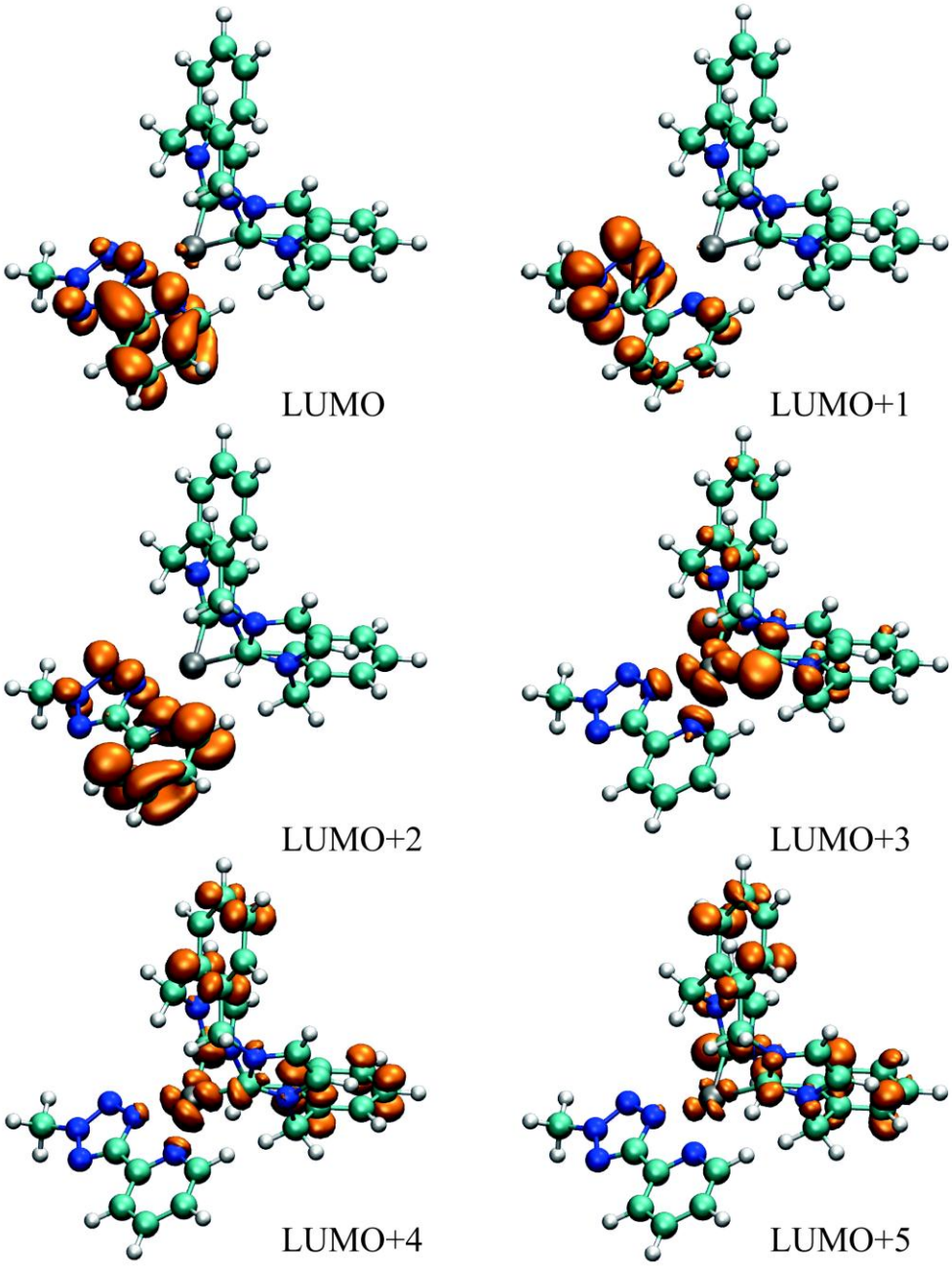

Selected unoccupied orbital representations for [Pt(**cyph**)(**pytetMe**)]$^{2+}$.

References

1. G. C. Crosby and J. N. Demas, *J Phys Chem-Us*, 1971, **75**, 991.
2. D. F. Eaton, *Pure and Applied Chemistry*, 1988, **60**, 1107.
3. M. J. Frisch, G. W. Trucks, H. B. Schlegel, G. E. Scuseria, M. A. Robb, J. R. Cheeseman, G. Scalmani, V. Barone, B. Mennucci, G. A. Patersson, H. Nakatsuji, M. Caricato, X. Li, H. P. Hratchian, A. F. Izmaylov, J. Bloino, G. Zheng, J. L. Sonnengerg, M. Hada, M. Ehara, K. Toyota, R. Fukuda, J. Hasegawa, M. Ishida, T. Nakajima, Y. Honda, O. Kitao, H. Nakai, T. Vreven, J. Montgomery, J. A., J. E. Peralta, F. Ogliaro, M. Bearpark, J. J. Heyd, E. Brothers, K. N. Kudin, V. N. Staroverov, R. Kobayashi, J. Normand, K. Raghavachari, A. Rendell, J. C. Burant, S. S. Iyengar, J. Tomasi, M. Cossi, N. Rega, J. M. Millam, M. Klene, J. E. Knox, J. B. Cross, V. Bakken, C. Adamo, J. Jaramillo, R. Gomperts, R. E. Stratmann, O. Yazyev, A. J. Austin, R. Cammi, C. Pomelli, J. W. Ochterski, R. L. Martin, K. Morokuma, V. G. Zakrzewski, G. A. Voth, P. Salvador, J. J. Dannenberg, S. Dapprich, A. D. Daniels, O. Farkas, J. B. Foresman, J. V. Ortiz, J. Cioslowski and D. J. Fox, *Gaussian 09, Revision B.01*, Wallingford CT, 2009.